State-of-the-art ab initio potential energy curve for the xenon atom pair and related spectroscopic and thermophysical properties

Robert Hellmann, Benjamin Jäger, and Eckard Bich

Citation: The Journal of Chemical Physics **147**, 034304 (2017); doi: 10.1063/1.4994267
View online: http://dx.doi.org/10.1063/1.4994267
View Table of Contents: http://aip.scitation.org/toc/jcp/147/3
Published by the American Institute of Physics

State-of-the-art *ab initio* potential energy curve for the xenon atom pair and related spectroscopic and thermophysical properties

Robert Hellmann,[a] Benjamin Jäger, and Eckard Bich
Institut für Chemie, Universität Rostock, 18059 Rostock, Germany

(Received 11 May 2017; accepted 5 July 2017; published online 21 July 2017)

A new *ab initio* interatomic potential energy curve for two ground-state xenon atoms is presented. It is based on supermolecular calculations at the coupled-cluster level with single, double, and perturbative triple excitations [CCSD(T)] employing basis sets up to sextuple-zeta quality, which were developed as part of this work. In addition, corrections were determined for higher coupled-cluster levels up to CCSDTQ as well as for scalar and spin-orbit relativistic effects at the CCSD(T) level. A physically motivated analytical function was fitted to the calculated interaction energies and used to compute the vibrational spectrum of the dimer, the second virial coefficient, and the dilute gas transport properties. The agreement with the best available experimental data for the investigated properties is excellent; the new potential function is superior not only to previous *ab initio* potentials but also to the most popular empirical ones. *Published by AIP Publishing.* [http://dx.doi.org/10.1063/1.4994267]

I. INTRODUCTION

Rare gases are important model substances for studying van der Waals interactions. This is not only because of the simple spherically symmetric nature of their pair potentials, which allows the use of highly accurate theoretical methods for the calculation of thermophysical and other properties, but also due to the applicability of high-level quantum-chemical *ab initio* approaches. For helium, thermophysical property values computed from the most accurate *ab initio* potential energy curves $V(R)$ are now more reliable than the best experimental data[1–4] and can therefore be used as calibration standards, e.g., for relative gas viscosity measurements.[5–7] For neon, our group developed a pair potential of reference quality,[8] and later we[9] as well as Patkowski and Szalewicz[10] thoroughly investigated the argon atom pair. Recently, highly accurate Kr–Kr potentials have been developed by Waldrop *et al.*[11] and by our group.[12] The derived thermophysical property data for gaseous neon,[13] argon,[4,14,15] and krypton[11,12] are again of reference quality. However, their estimated uncertainties are considerably larger than those for helium because the potential energy curve of the four-electron He–He system can be determined much more accurately than the potential energy curves of the heavier rare gas pairs.

Interactions between two ground-state xenon atoms have been investigated by means of *ab initio* methods in several studies, see, for example, Refs. 16–21. However, to the best of our knowledge, only the papers of Slavíček *et al.*[19] and of Hanni *et al.*[20] dealt with wide ranges of interatomic separations and provided analytical potential functions. These two groups determined the individual interaction energies using the counterpoise-corrected supermolecular approach[22] at the coupled-cluster level with single, double, and perturbative triple excitations [CCSD(T)][23] using a pseudopotential (PP) to account for relativistic effects and PP basis sets up to quadruple-zeta quality with bond functions. Hanni *et al.* also applied a core-polarization potential (CPP) to account for core-valence correlation effects. The potential of Slavíček *et al.* features a well depth of D_e = 263.42 K, whereas that of Hanni *et al.* is considerably deeper, D_e = 283.06 K, which is mainly due to the use of the CPP. The latter value is close to those for the popular empirical potential curves of Aziz and Slaman[24] (D_e = 282.29 K) and of Dham *et al.*[25] (D_e = 282.80 K), which were fitted to the best available experimental data for several related properties.

In this work, we present a new Xe–Xe potential energy curve, which is based on counterpoise-corrected supermolecular coupled-cluster calculations up to the CCSDTQ[26,27] level for a large number of interatomic separations R. Corrections for scalar, spin-(own)-orbit, and spin-other-orbit relativistic effects were computed at the CCSD(T) level. For all supermolecular calculations, we employed newly developed nonrelativistic gaussian basis sets up to sextuple-zeta quality, which are also presented in this paper. An analytical function was fitted to the calculated interaction energies and used to compute the vibrational spectrum of the xenon dimer as well as the second virial coefficient and the dilute gas transport properties of xenon in the temperature range from 100 K to 5000 K.

In Sec. II, we summarize the development of the new gaussian basis sets for xenon. The *ab initio* calculations and results for the Xe–Xe interaction energies are presented in Sec. III, followed in Sec. IV by the discussion of the analytical potential function and of the computed vibrational spectrum. In Sec. V, we compare the calculated values of the thermophysical properties of dilute xenon gas with experimental data. A summary and conclusions are given in Sec. VI.

II. GAUSSIAN BASIS SETS FOR XENON

In our previous work on the Ne–Ne,[8] Ar–Ar,[9] and Kr–Kr[12] systems, we used correlation-consistent (cc) basis sets[28–37] up to polarized-valence sextuple-zeta size (abbreviated here as

[a]Electronic mail: robert.hellmann@uni-rostock.de

V6Z) to reach the desired accuracy for the interaction energies. For krypton, we developed the V6Z basis set as part of our study.[12] When we started the present work on the xenon atom pair, cc basis sets for xenon were only available for PP calculations.[38] However, employing a PP approach limits the accuracy that can be achieved for the potential energy curve. Hence, we decided to construct standard (i.e., all-electron) VDZ to V6Z basis sets for xenon from scratch in a systematic manner to ensure smooth extrapolation behavior of the calculated interaction energy contributions to the complete basis set (CBS) limit. The methodology described below is loosely based on that of the cc basis sets. Note that standard cc basis sets for xenon up to quadruple-zeta quality have recently been published by two research groups.[39,40] The cc basis sets of Bross and Peterson[39] were optimized for scalar relativistic calculations, whereas those of Mahler and Wilson[40] were optimized nonrelativistically. The latter use very few primitive functions for the atomic Hartree–Fock self-consistent-field (SCF) orbitals in order to improve computational efficiency when using uncontracted basis sets, which is common in relativistic calculations. In the present work, we have only used our own basis sets, which are indicated by a prime (′) to distinguish them from the cc sets.

In the first step, we optimized the exponents of five primitive sets, $(23s16p9d)$, $(25s18p11d)$, $(27s20p13d)$, $(29s22p15d)$, and $(31s24p17d)$, by minimizing the atomic SCF energy. These primitive sets, which are much larger than those of Mahler and Wilson,[40] were then contracted to $[5s4p2d]$, i.e., each atomic orbital is represented by a single contracted basis function.

The VDZ′, VTZ′, VQZ′, V5Z′, and V6Z′ basis sets were obtained by adding a $(1s1p1d)$ set to the $(23s16p9d)/[5s4p2d]$ set, a $(2s2p2d1f)$ set to the $(25s18p11d)/[5s4p2d]$ set, a $(3s3p3d2f1g)$ set to the $(27s20p13d)/[5s4p2d]$ set, a $(4s4p4d3f2g1h)$ set to the $(29s22p15d)/[5s4p2d]$ set, and a $(5s5p5d4f3g2h1i)$ set to the $(31s24p17d)/[5s4p2d]$ set, respectively. The exponents of functions of the same type (symmetry) were chosen to be even-tempered, resulting in 3 (VDZ′) to 13 (V6Z′) adjustable parameters, which were optimized by minimizing the atomic energy at the configuration interaction with single and double excitations (CISD) level of theory within the frozen-core (FC) approximation (only $5s$ and $5p$ electrons correlated).

Augmented basis sets, denoted as aV$XZ′$ with $X \in \{\mathrm{D}, \mathrm{T}, \mathrm{Q}, 5, 6\}$, were constructed by adding one primitive function of each type. The exponents were obtained by simply multiplying the exponent of the most diffuse function of each type by a factor of 0.5. Doubly augmented sets, daV$XZ′$, were obtained from the aV$XZ′$ sets in the same manner.

Core-valence basis sets, CV$XZ′$ with $X \in \{\mathrm{D}, \mathrm{T}, \mathrm{Q}\}$, were constructed by adding a $(1s1p1d2f1g)$ set to VDZ′, a $(2s2p2d3f2g1h)$ set to VTZ′, and a $(3s3p3d4f3g2h1i)$ set to VQZ′. The exponents of functions of the same type were again chosen to be even-tempered. The resulting adjustable parameters were optimized by minimizing the atomic energy at the CISD level of theory with an inner core consisting of the $1s$, $2s$, $2p$, $3s$, $3p$, and $3d$ electrons treated as frozen (denoted as IFC approximation). The previously optimized valence exponents of the V$XZ′$ basis sets were not altered during the optimization. To obtain aCV$XZ′$ and daCV$XZ′$ basis sets, the diffuse functions of the respective aV$XZ′$ and daV$XZ′$ basis sets were added.

Uncontracted versions of the aV$XZ′$ (with $X \leqslant 5$) and aCV$XZ′$ basis sets, denoted as uaV$XZ′$ and uaCV$XZ′$, respectively, were also used in this work. However, to avoid near-linear dependencies in the basis sets, all primitive s, p, and d functions that were added to the initially optimized SCF sets were removed and replaced by $(1s1p2d)$ sets, whose exponents were determined from the lowest s, p, and d exponents in the SCF sets by multiplying them by 0.5 for the s and p functions and by 0.5 and 0.25 for the d functions.

For all-electron (AE) correlation calculations, additional $(2f2g)$ and $(2f2g2h)$ sets were added to the uaCVDZ′ and uaCVTZ′ basis sets, respectively. The two additional functions of each type were generated by multiplying the highest respective exponents in the uaCVDZ′ and uaCVTZ′ basis sets by factors of 3 and 9. The resulting sets are denoted as uaCVDZmod′ and uaCVTZmod′.

The NWChem[41] and PSI3[42] programs were employed for the development of the basis sets. The exponents and contraction coefficients of all basis sets are provided in the supplementary material.

III. CALCULATION OF INTERACTION ENERGIES

All Xe–Xe interaction energies presented in this work were calculated using the supermolecular approach including the full counterpoise correction.[22] In most of the calculations, we supplemented the atomic basis sets by a $(4s4p3d3f2g)$ or $(3s3p2d1f)$ set of bond functions located in the center of the atom pair, which greatly reduces the basis set incompleteness error. The larger set, denoted as bf1, is characterized by exponents of 0.06, 0.18, 0.54, and 1.62 for the s and p functions, 0.15, 0.45, and 1.35 for the d and f functions, and 0.3 and 0.9 for the g functions. The exponents of the smaller set, which is denoted as bf2, are 0.1, 0.3, and 0.9 for the s and p functions, 0.25 and 0.75 for the d functions, and 0.45 for the f function.

Extrapolation of the correlation part of the interaction energy to the CBS limit was conducted by means of the two-point scheme recommended by Halkier *et al.*,[43]

$$V_{\mathrm{corr}}^{\mathrm{CBS}} = \frac{l_{\mathrm{max}}^3 V_{\mathrm{corr}}^{l_{\mathrm{max}}} - (l_{\mathrm{max}} - 1)^3 V_{\mathrm{corr}}^{l_{\mathrm{max}}-1}}{l_{\mathrm{max}}^3 - (l_{\mathrm{max}} - 1)^3}, \tag{1}$$

where l_{max} is the highest angular momentum quantum number in the larger of the two basis sets. Thus, we have $l_{\mathrm{max}} = X + 2$ for the core-valence basis sets and $l_{\mathrm{max}} = X$ otherwise. The SCF contribution was not extrapolated because it converges much faster to the CBS limit than the correlation contribution. Therefore, the total interaction energy in the CBS limit was approximated as the sum of the extrapolated correlation contribution and the SCF contribution obtained using the larger basis set. We also applied Eq. (1) for the CBS extrapolation of correlation energy differences between two levels of theory as well as for the CBS extrapolation of the relativistic corrections. The latter also have SCF contributions, which are, however, only very weakly dependent on X. Thus, extrapolation of the total relativistic corrections yields almost the same results as extrapolation of only their correlation parts. Note that using the same

set of bond functions for both basis set levels in Eq. (1) does not appear to significantly affect the approximate proportionality of the basis set incompleteness error to $l_{\max}^{-3}$ (on which this extrapolation scheme is based) for the Xe–Xe correlation interaction energy contributions.

The interaction energy was determined at 39 separations R in the range from 2.4 Å to 15 Å as the sum of three major contributions,

$$V_{\text{total}} = V_{\text{CCSD(T)}} + V_{\text{rel-CCSD(T)}} + V_{\text{post-CCSD(T)}}, \quad (2)$$

where $V_{\text{CCSD(T)}}$, $V_{\text{rel-CCSD(T)}}$, and $V_{\text{post-CCSD(T)}}$ denote the nonrelativistic CCSD(T) interaction energy, its relativistic correction, and the nonrelativistically calculated contribution of higher coupled-cluster terms up to CCSDTQ, respectively. We discuss each of the three contributions in the following subsections. All interaction energies and their individual contributions are given in Kelvin, i.e., as V/k_{B}, where the Boltzmann constant k_{B} is omitted for brevity.

A. Nonrelativistic CCSD(T) interaction energy

The nonrelativistic CCSD(T) interaction energy was treated as the sum of four terms,

$$V_{\text{CCSD(T)}} = V_{\text{SCF}} + V_{\text{corr/FC}} + V_{\text{IFC–FC}} + V_{\text{AE–IFC}}. \quad (3)$$

The terms V_{SCF} and $V_{\text{corr/FC}}$ denote the SCF part and the correlation contribution within the FC approximation, respectively. They were calculated using daVXZ' basis sets supplemented by the bf1 set of bond functions. The resulting interaction energy contributions are denoted as $V_{\text{SCF}}^{\text{daV}XZ'\text{+bf1}}$ and $V_{\text{corr/FC}}^{\text{daV}XZ'\text{+bf1}}$. The latter was extrapolated to the CBS limit using the results for $X=5$ and $X=6$, with the CBS value being denoted as $V_{\text{corr/FC}}^{\text{daV(56)Z'+bf1}}$. At $R=4.4$ Å, which is close to the minimum of the potential energy curve, we obtained $V_{\text{SCF}}^{\text{daV5Z'+bf1}} = 294.69$ K, $V_{\text{SCF}}^{\text{daV6Z'+bf1}} = 294.57$ K, $V_{\text{corr/FC}}^{\text{daV5Z'+bf1}} = -547.03$ K, $V_{\text{corr/FC}}^{\text{daV6Z'+bf1}} = -548.20$ K, and $V_{\text{corr/FC}}^{\text{daV(56)Z'+bf1}} = -549.80$ K. This shows that, in contrast to the correlation contribution, the SCF part is sufficiently well converged at the $X = 6$ basis set level and does not need to be extrapolated. At very small interatomic separations, $R \leqslant 2.8$ Å, we had to use the singly augmented basis sets due to near-linear dependencies. However, at $R = 3.0$ Å, the smallest distance at which calculations with the doubly augmented sets could be successfully performed, this affects the total interaction energy, $V_{\text{FC}}^{\text{(d)aV(56)Z'+bf1}} = V_{\text{SCF}}^{\text{(d)aV6Z'+bf1}} + V_{\text{corr/FC}}^{\text{(d)aV(56)Z'+bf1}}$, by only 0.012%.

The third term in Eq. (3), $V_{\text{IFC–FC}}$, denotes the correction for core-core and core-valence correlation effects arising from including also the 4s, 4p, and 4d electrons in the correlation treatment (IFC approximation). It was computed as the CBS extrapolated difference between the CCSD(T) interaction energies at the IFC and FC levels obtained using the daCVTZ'+bf2 and daCVQZ'+bf2 basis sets. For the test geometry $R = 4.4$ Å, this yields $V_{\text{IFC–FC}}^{\text{daCVTZ'+bf2}} = -21.15$ K, $V_{\text{IFC–FC}}^{\text{daCVQZ'+bf2}} = -21.07$ K, and $V_{\text{IFC–FC}}^{\text{daCV(TQ)Z'+bf2}} = -20.96$ K.

The final term in Eq. (3), $V_{\text{AE–IFC}}$, denotes the correction arising from including all electrons in the correlation treatment that were not already included at the IFC level. This term was calculated using the uaCVDZmod'+bf2 and uaCVTZmod'+bf2 basis sets and was also extrapolated to the CBS limit. At $R = 4.4$ Å, we obtained $V_{\text{AE–IFC}}^{\text{uaCVDZmod'+bf2}} = -0.346$ K, $V_{\text{AE–IFC}}^{\text{uaCVTZmod'+bf2}} = -0.353$ K, and $V_{\text{AE–IFC}}^{\text{uaCV(DT)Zmod'+bf2}} = -0.360$ K, yielding $V_{\text{CCSD(T)}} = -276.55$ K. All terms contributing to $V_{\text{CCSD(T)}}$ were computed using the CFOUR program.[44]

B. Relativistic correction

We determined the relativistic correction to the Xe–Xe interaction energy at the CCSD(T) level of theory using the same basic approach as in our study of the Kr–Kr potential,[12]

$$V_{\text{rel-CCSD(T)}} = V_{\text{DPT2/FC}} + V_{\text{DPT2/IFC–FC}} + V_{\text{4cDC–DPT2/FC}} + V_{\text{Gaunt/FC}}. \quad (4)$$

The terms $V_{\text{DPT2/FC}}$ and $V_{\text{DPT2/IFC–FC}}$ denote the scalar relativistic correction determined by means of second-order direct perturbation theory (DPT2)[45,46] within the FC approximation and its correction for core-core and core-valence correlation effects at the IFC level, respectively. Both terms were calculated using uncontracted basis sets. At $R = 4.4$ Å, we obtained $V_{\text{DPT2/FC}}^{\text{uaVQZ'+bf2}} = -11.09$ K, $V_{\text{DPT2/FC}}^{\text{uaV5Z'+bf2}} = -10.46$ K, and $V_{\text{DPT2/FC}}^{\text{uaV(Q5)Z'+bf2}} = -9.79$ K as well as $V_{\text{DPT2/IFC–FC}}^{\text{uaCVTZ'+bf2}} = 0.96$ K, $V_{\text{DPT2/IFC–FC}}^{\text{uaCVQZ'+bf2}} = 0.91$ K, and $V_{\text{DPT2/IFC–FC}}^{\text{uaCV(TQ)Z'+bf2}} = 0.85$ K.

The term $V_{\text{4cDC–DPT2/FC}}$ denotes the difference between the interaction energies obtained from four-component Dirac–Coulomb and DPT2 computations within the FC approximation and accounts mainly for spin-(own)-orbit effects. Using again uncontracted basis sets, we obtained $V_{\text{4cDC–DPT2/FC}}^{\text{uaVDZ'+bf2}} = -2.03$ K, $V_{\text{4cDC–DPT2/FC}}^{\text{uaVTZ'+bf2}} = -2.36$ K, and $V_{\text{4cDC–DPT2/FC}}^{\text{uaV(DT)Z'+bf2}} = -2.50$ K for the test geometry.

The last term in Eq. (4), $V_{\text{Gaunt/FC}}$, is the Gaunt (spin-other-orbit) contribution. It was determined by taking the difference between interaction energies calculated with the four-component Dirac–Coulomb–Gaunt and Dirac–Coulomb Hamiltonians within the molecular mean-field approximation (see Ref. 47 and references therein) at the FC level. We used the same basis sets as for $V_{\text{4cDC–DPT2/FC}}$, yielding $V_{\text{Gaunt/FC}}^{\text{uaVDZ'+bf2}} = -0.27$ K, $V_{\text{Gaunt/FC}}^{\text{uaVTZ'+bf2}} = -0.43$ K, and $V_{\text{Gaunt/FC}}^{\text{uaV(DT)Z'+bf2}} = -0.49$ K at $R = 4.4$ Å. The resulting total relativistic correction $V_{\text{rel-CCSD(T)}}$ at this separation is −11.94 K.

The four-component computations were performed using the DIRAC program[48] with explicit calculation of the two-electron (SS|SS) integrals over the small component. All other calculations pertaining to $V_{\text{rel-CCSD(T)}}$ were carried out using CFOUR.[44]

C. Post-CCSD(T) contributions

The correction for higher coupled-cluster levels up to CCSDTQ was calculated as the sum of five terms,

$$V_{\text{post-CCSD(T)}} = V_{\text{T–(T)/FC}} + V_{\text{(Q)–T/FC}} + V_{\text{Q–(Q)/FC}} + V_{\text{T–(T)/IFC'–FC}} + V_{\text{(Q)–T/IFC'–FC}}. \quad (5)$$

The first three terms, $V_{\text{T–(T)/FC}}$, $V_{\text{(Q)–T/FC}}$, and $V_{\text{Q–(Q)/FC}}$, denote the differences between the CCSDT[49] and CCSD(T)

levels, the CCSDT(Q)[50] and CCSDT levels, and the CCSDTQ and CCSDT(Q) levels, respectively, within the FC approximation. For $V_{\mathrm{T-(T)/FC}}$ at $R = 4.4$ Å, we obtained $V^{\mathrm{daVQZ'+bf2}}_{\mathrm{T–(T)/FC}} = 5.97$ K, $V^{\mathrm{daV5Z'+bf2}}_{\mathrm{T–(T)/FC}} = 6.40$ K, and $V^{\mathrm{daV(Q5)Z'+bf2}}_{\mathrm{T–(T)/FC}} = 6.85$ K. The results for $V_{\mathrm{(Q)-T/FC}}$ at this separation are $V^{\mathrm{aVTZ'+bf2}}_{\mathrm{(Q)–T/FC}} = -3.80$ K, $V^{\mathrm{aVQZ'+bf2}}_{\mathrm{(Q)–T/FC}} = -4.45$ K, and $V^{\mathrm{aV(TQ)Z'+bf2}}_{\mathrm{(Q)–T/FC}} = -4.93$ K, and those for $V_{\mathrm{Q-(Q)/FC}}$, which could only be computed using basis sets up to aVTZ′ without bond functions, are $V^{\mathrm{aVDZ'}}_{\mathrm{Q–(Q)/FC}} = 0.56$ K, $V^{\mathrm{aVTZ'}}_{\mathrm{Q–(Q)/FC}} = -0.21$ K, and $V^{\mathrm{aV(DT)Z'}}_{\mathrm{Q–(Q)/FC}} = -0.54$ K. We also computed the difference between the CCSDTQ(P)[51] and CCSDTQ levels of theory for the test geometry using the aVDZ′ basis set. The resulting correction of −0.05 K can only be regarded as a rough estimate, and the behavior might be different for other interatomic distances. Nevertheless, it provides strong evidence that the coupled-cluster series truncated at the CCSDTQ level is sufficiently converged.

The terms $V_{\mathrm{T–(T)/IFC'–FC}}$ and $V_{\mathrm{(Q)–T/IFC'–FC}}$ correct the terms $V_{\mathrm{T-(T)/FC}}$ and $V_{\mathrm{(Q)-T/FC}}$ for the inclusion of the 4*d* electrons in the correlation treatment (denoted as IFC′ approximation). It was not possible to use the IFC approximation in post-CCSD(T) calculations due to the very high computational costs. However, at the CCSD(T) level, the IFC and IFC′ approximations yield very similar results (as already noted by Shee *et al.*[21]). For $V_{\mathrm{T–(T)/IFC'–FC}}$ at $R = 4.4$ Å, we obtained surprisingly large values, $V^{\mathrm{aCVDZ'+bf2}}_{\mathrm{T–(T)/IFC'–FC}} = 6.64$ K, $V^{\mathrm{aCVTZ'+bf2}}_{\mathrm{T–(T)/IFC'–FC}} = 8.40$ K, and $V^{\mathrm{aCV(DT)Z'+bf2}}_{\mathrm{T–(T)/IFC'–FC}} = 10.25$ K. The term $V_{\mathrm{(Q)-T/FC}}$ could only be computed at the aCVDZ′+bf2 level, making it the only post-SCF contribution to the potential energy curve that could not be extrapolated to the CBS limit. For the test geometry, we obtained $V^{\mathrm{aCVDZ'+bf2}}_{\mathrm{(Q)–T/IFC'–FC}} = -2.79$ K. The resulting post-CCSD(T) correction $V_{\mathrm{post\text{-}CCSD(T)}}$ at $R = 4.4$ Å is 8.85 K.

The CCSDT, CCSDT(Q), and CCSDTQ calculations were performed using either the new NCC module of CFOUR[44,52] or the MRCC code.[53] The latter was also used for the CCSDTQ(P) test calculations. All CCSD(T) calculations needed to determine the post-CCSD(T) corrections were performed using CFOUR.

D. Uncertainty budget

The combined uncertainties of the *ab initio* interaction energies V_{total} were determined as the square roots of the sums of the squared uncertainties resulting from the individual contributions in accordance with the standard procedure for the evaluation of measurement uncertainties. We estimated the uncertainties of contributions that were extrapolated to the CBS limit as half the absolute values of the differences between the CBS extrapolated values and the values resulting for the basis set with the highest cardinal number X. For V_{SCF}, we used the absolute values of the differences between the $X = 6$ and $X = 5$ levels, and for $V_{\mathrm{(Q)–T/IFC'–FC}}$, we assumed a relative uncertainty of 50%. To account for the neglect of relativistic corrections to the post-CCSD(T) terms and other neglected contributions, we increased the resulting estimate of the combined uncertainty of V_{total} by a further 25%.

In the case of the Kr–Kr potential,[12] we regarded the combined uncertainties resulting from a similar procedure as standard uncertainties, corresponding approximately to a 68% confidence level. However, based on the analysis of the quality of the new Xe–Xe potential given in Secs. IV and V, we regard the present estimates as expanded uncertainties with coverage

TABLE I. Individual contributions to the Xe–Xe interaction energy, see Eqs. (2)–(5), and their estimated uncertainties at $R = 3.2$ Å, $R = 4.4$ Å, and $R = 6.0$ Å. All energies are in Kelvin.

		$R = 3.2$ Å		$R = 4.4$ Å		$R = 6.0$ Å	
Contribution	Basis set level	Value	Uncertainty	Value	Uncertainty	Value	Uncertainty
SCF	daV6Z′+bf1	10015.13	11.94	294.57	0.12	1.85	0.00
Corr/FC	daV(56)Z′+bf1	−3404.69	19.35	−549.80	0.80	−64.60	0.04
IFC–FC	daCV(TQ)Z′+bf2	−480.07	17.10	−20.96	0.06	−0.61	0.08
AE–IFC	uaCV(DT)Zmod′+bf2	−11.91	0.43	−0.36	0.00	0.02	0.00
CCSD(T)		6118.46	28.46	−276.55	0.81	−63.34	0.09
DPT2/FC	uaV(Q5)Z′+bf2	−782.86	3.06	−9.79	0.33	2.00	0.03
DPT2/IFC–FC	uaCV(TQ)Z′+bf2	15.04	0.44	0.85	0.03	−0.07	0.00
4cDC–DPT2/FC	uaV(DT)Z′+bf2	−22.11	0.43	−2.50	0.07	−0.66	0.01
Gaunt/FC	uaV(DT)Z′+bf2	24.81	0.23	−0.49	0.03	−0.25	0.00
Rel-CCSD(T)		−765.12	3.13	−11.94	0.34	1.03	0.03
T–(T)/FC	daV(Q5)Z′+bf2	39.62	1.12	6.85	0.23	0.93	0.03
(Q)–T/FC	aV(TQ)Z′+bf2	−27.73	1.14	−4.93	0.24	−0.61	0.04
Q–(Q)/FC	aV(DT)Z′	−1.24	0.65	−0.54	0.16	−0.10	0.03
T–(T)/IFC′–FC	aCV(DT)Z′+bf2	52.26	5.19	10.25	0.93	1.33	0.12
(Q)–T/IFC′–FC	aCVDZ′+bf2	−11.36	5.68	−2.79	1.39	−0.41	0.21
Post-CCSD(T)		51.55	7.89	8.85	1.71	1.14	0.24
Total		5404.88	37.12	−279.63	2.41	−61.18	0.33

TABLE II. Total Xe–Xe interaction energy, its estimated uncertainty, the interaction energy resulting from the fitted analytical function, and the difference between the fitted and calculated interaction energy as a function of the interatomic distance. All energies are in Kelvin.

R/Å	V_{total}	$u(V_{\text{total}})$	V_{fit}	$V_{\text{fit}} - V_{\text{total}}$
2.4	67 031.245	409.930	67 028.080	−3.165
2.6	37 578.501	209.222	37 582.273	3.772
2.8	20 522.124	112.767	20 521.635	−0.489
3.0	10 810.352	63.434	10 809.878	−0.474
3.2	5 404.877	37.123	5 404.520	−0.357
3.4	2 481.019	22.141	2 480.950	−0.069
3.5	1 592.042	17.185	1 592.036	−0.006
3.6	958.642	13.388	958.744	0.102
3.7	514.265	10.482	514.368	0.103
3.8	208.418	8.250	208.529	0.111
3.9	3.312	6.537	3.391	0.079
4.0	−129.334	5.221	−129.296	0.038
4.1	−210.472	4.214	−210.487	−0.015
4.2	−255.560	3.444	−255.616	−0.056
4.3	−275.892	2.858	−275.965	−0.073
4.4	−279.634	2.408	−279.700	−0.066
4.5	−272.638	2.056	−272.678	−0.040
4.6	−259.034	1.774	−259.045	−0.011
4.7	−241.706	1.544	−241.693	0.013
4.8	−222.630	1.352	−222.601	0.029
4.9	−203.141	1.189	−203.090	0.051
5.0	−184.042	1.050	−184.015	0.027
5.2	−149.040	0.824	−149.030	0.010
5.4	−119.495	0.651	−119.491	0.004
5.6	−95.464	0.516	−95.464	0.000
5.8	−76.301	0.410	−76.309	−0.008
6.0	−61.180	0.327	−61.190	−0.010
6.2	−49.288	0.262	−49.300	−0.012
6.4	−39.932	0.211	−39.947	−0.015
6.6	−32.569	0.170	−32.568	0.001
6.9	−24.262	0.126	−24.260	0.002
7.2	−18.336	0.094	−18.324	0.012
7.5	−14.034	0.072	−14.025	0.009
8.0	−9.223	0.048	−9.225	−0.002
8.5	−6.248	0.033	−6.251	−0.003
9.0	−4.343	0.023	−4.345	−0.002
10.0	−2.237	0.012	−2.239	−0.002
12.0	−0.724	0.004	−0.723	0.001
15.0	−0.184	0.001	−0.184	0.000

factor $k = 2$, corresponding approximately to a 95% confidence level.

Table I lists the individual contributions to the interaction energy and their estimated uncertainties at three interatomic distances. The total interaction energies and their uncertainties for all 39 investigated interatomic separations are given in Table II. Detailed results for the individual contributions at all separations are provided in the supplementary material.

IV. ANALYTICAL POTENTIAL FUNCTION AND VIBRATIONAL SPECTRUM OF THE XENON DIMER

A modified Tang–Toennies potential function[54] was fitted to the 39 calculated interaction energies V_{total},

$$V(R) = A \exp\left(a_1 R + a_2 R^2 + a_{-1} R^{-1} + a_{-2} R^{-2}\right) - \sum_{n=3}^{8} \frac{C_{2n}}{R^{2n}} \left[1 - \exp(-bR) \sum_{k=0}^{2n} \frac{(bR)^k}{k!}\right]. \quad (6)$$

The parameters A, a_1, a_2, a_{-1}, a_{-2}, and b as well as the dispersion coefficients C_6, C_8, and C_{10} were treated as independent fit parameters, whereas the higher dispersion coefficients C_{12}, C_{14}, and C_{16} were tied to the lower ones by an approximate recursion formula,[54]

$$C_{2n} = C_{2n-6}\left(\frac{C_{2n-2}}{C_{2n-4}}\right)^3, \qquad n \geq 6. \quad (7)$$

The interaction energies computed using the analytical function at all 39 investigated separations R as well as their deviations from V_{total} are provided in Table II, while the optimized values of the potential parameters are listed in Table III. Additional sets of parameters were determined from fits to interaction energies perturbed by adding or subtracting the uncertainty estimates at each separation, $V_{\text{U1}} = V_{\text{total}} + u(V_{\text{total}})$ and $V_{\text{U2}} = V_{\text{total}} - u(V_{\text{total}})$. Two further potential energy curves, V_{U3} and V_{U4}, were obtained in a similar manner as V_{U1} and V_{U2}, respectively, but with $u(V_{\text{total}})$ at $R < 5$ Å multiplied by $-\cos[\pi(R/\text{Å} - 2.4)/(5.0 - 2.4)]$. Thus, $V_{\text{U3}} = V_{\text{U1}}$ and $V_{\text{U4}} = V_{\text{U2}}$ for $R \geqslant 5$ Å, but $V_{\text{U3}} = V_{\text{U2}}$ and $V_{\text{U4}} = V_{\text{U1}}$ at $R = 2.4$ Å. The crossing of V_{U3} and V_{U4} (i.e., $V_{\text{U3}} = V_{\text{U4}} = V_{\text{total}}$) occurs at $R = 3.7$ Å. The parameters of the perturbed potentials are provided in the supplementary material.

TABLE III. Parameters of the fitted analytical potential function, C_6 and C_8 dispersion coefficients from the literature,[16,19,20,55] and well depth and equilibrium bond length of the present potential function and values from the literature.[19–21,24,25,56]

Parameter	Unit	Value	Lit. values	Reference
A	K	$0.579\,317\,071 \times 10^8$		
a_1	Å^{-1}	$-0.208\,311\,994 \times 10^1$		
a_2	Å^{-2}	−0.147 746 919		
a_{-1}	Å	$-0.289\,687\,722 \times 10^1$		
a_{-2}	Å^2	$0.258\,976\,595 \times 10^1$		
b	Å^{-1}	$0.244\,337\,880 \times 10^1$		
C_6	K Å^6	$0.200\,298\,034 \times 10^7$	$0.199\,98 \times 10^7$	16
			$0.197\,21 \times 10^7$	19
			$0.197\,34 \times 10^7$	20
			$0.199\,35 \times 10^7$	55
C_8	K Å^8	$0.199\,130\,481 \times 10^8$	$0.221\,16 \times 10^8$	16
			$0.235\,92 \times 10^8$	20
C_{10}	K Å^{10}	$0.286\,841\,040 \times 10^9$		
D_e	K	279.975	282.29	24
			282.80	25
			263.42	19
			283.06	20
			300.95	21
R_e	Å	4.377 98	4.3627	24
			4.3656	25
			4.4213	19
			4.3818	20
			4.3773	56
			4.347	21

The well depth of the present potential energy curve is $D_e = (279.98 \pm 2.52)$ K, where the uncertainty was determined from the perturbed potentials. The equilibrium bond length is $R_e = (4.3780 \pm 0.0036)$ Å, which is in almost perfect agreement with the experimental value $R_e = (4.3773 \pm 0.0049)$ Å determined from the rotational constants of the vibrational states $v = 0$ and $v = 1$ of the dimer ^{129}Xe–^{132}Xe by Wüest *et al.*[56] Our values for D_e and R_e are also in close agreement with those of the empirical potentials of Aziz and Slaman[24] ($D_e = 282.29$ K, $R_e = 4.3627$ Å) and of Dham *et al.*[25] ($D_e = 282.80$ K, $R_e = 4.3656$ Å) as well as with those of the *ab initio* potential of Hanni *et al.*[20] ($D_e = 283.06$ K, $R_e = 4.3818$ Å). Further selected results from the literature for these two parameters[19,21] and for the C_6 and C_8 dispersion coefficients[16,19,20,55] are given in Table III. The reference value for C_6 is that of Kumar and Thakkar,[55] which was determined with an uncertainty of 1% from the dipole oscillator strength distribution (DOSD) and differs from our fitted value by only –0.47%.

As a further test of the quality of the new potential, the spacings $\Delta G_{v+1/2}$ between the vibrational states v and $v + 1$ for the electronic and rotational ground state of the xenon dimer were calculated by solving the one-dimensional radial Schrödinger equation using the LEVEL program (version 7.7) of Le Roy.[57] The only experimental data available for $\Delta G_{v+1/2}$ over a larger range of v values are those of Freeman *et al.*,[58] which were measured up to $v = 9$ and could not be isotopically resolved. For consistency with their data, we calculated the $\Delta G_{v+1/2}$ values for all 45 combinations of the nine naturally occurring isotopes and averaged the results,

$$\langle \Delta G_{v+1/2} \rangle = \sum_i x_i^2 \Delta G_{v+1/2;i,i} + 2 \sum_{i<j} x_i x_j \Delta G_{v+1/2;i,j}, \quad (8)$$

where x_i is the mole fraction of the ith isotope in naturally occurring xenon.[59] A calculation for a hypothetical dimer with atomic masses corresponding to the average isotopic mass (131.293 u) yields $\Delta G_{v+1/2}$ values that differ from those obtained using Eq. (8) by at most 0.01% for $v \leqslant 9$. The results for the present potential (with uncertainties estimated utilizing V_{U1} to V_{U4}) and for the potentials of Aziz and Slaman,[24] of Dham *et al.*,[25] of Slavíček *et al.*,[19] and of Hanni *et al.*[20] are listed along with the data of Freeman *et al.* in Table IV. The uncertainties of the present results are more than three times smaller than those of the experimental data. For $v \geqslant 2$, the agreement is within (and for $v = 1$ almost within) the mutual uncertainty, but the disagreement for $v = 0$ between our value, $\langle \Delta G_{1/2} \rangle = (19.31 \pm 0.08)$ cm^{-1}, and that of Freeman *et al.*, $\langle \Delta G_{1/2} \rangle = (19.90 \pm 0.3)$ cm^{-1}, is striking. However, our value is fully consistent with the extremely accurate value of Wüest *et al.*,[56] $\langle \Delta G_{1/2} \rangle = (19.3485 \pm 0.0005)$ cm^{-1}, which is based on measurements of $\Delta G_{1/2}$ for the dimers ^{129}Xe–^{132}Xe and ^{131}Xe–^{136}Xe converted to the isotopically averaged value by means of a potential model, see Ref. 56 for details. Aziz and Slaman[24] and Dham *et al.*[25] employed the data of Freeman *et al.* (the measurements of Wüest *et al.* were not yet available at the time) in the multi-property fits of their potentials, which both yield $\langle \Delta G_{1/2} \rangle = 19.61$ cm^{-1}. The *ab initio* potential of Hanni *et al.*[20] yields $\langle \Delta G_{v+1/2} \rangle$ values that almost fall within the uncertainty ranges of our values, whereas the values obtained using the *ab initio* potential of Slavíček *et al.*[19] are systematically too small due to the potential well being too shallow. The $\Delta G_{v+1/2}$ values obtained using the present potential for all 45 isotopic combinations are provided in the supplementary material.

TABLE IV. Isotopically averaged vibrational spacings $\langle \Delta G_{v+1/2} \rangle$ (in cm^{-1}) of the xenon dimer up to $v = 9$ for the potential energy curves of the present work, of Aziz and Slaman,[24] of Dham *et al.*,[25] of Slavíček *et al.*,[19] and of Hanni *et al.*[20] The experimental values are those of Freeman *et al.*[58]

		Literature potentials				Experiment
v	This work	Ref. 24	Ref. 25	Ref. 19	Ref. 20	Ref. 58
0	19.31 ± 0.08	19.61	19.61	18.69	19.39	19.90 ± 0.3
1	18.15 ± 0.08	18.41	18.45	17.53	18.23	18.55 ± 0.3
2	16.99 ± 0.09	17.21	17.28	16.37	17.08	17.20 ± 0.3
3	15.83 ± 0.09	16.02	16.09	15.21	15.93	16.17 ± 0.3
4	14.68 ± 0.09	14.83	14.89	14.07	14.79	14.63 ± 0.3
5	13.54 ± 0.09	13.66	13.71	12.92	13.65	13.70 ± 0.3
6	12.41 ± 0.09	12.50	12.54	11.79	12.52	12.63 ± 0.3
7	11.29 ± 0.09	11.35	11.40	10.68	11.41	11.33 ± 0.3
8	10.19 ± 0.09	10.23	10.27	9.58	10.32	10.15 ± 0.3
9	9.12 ± 0.09	9.14	9.16	8.51	9.25	8.95 ± 0.3

V. THERMOPHYSICAL PROPERTIES OF DILUTE XENON GAS

A. Second virial coefficient

The second virial coefficient B_2 was computed semiclassically as the sum of the classical contribution and the first- and second-order quantum corrections,

$$B_2(T) = B_2^{\mathrm{cl}}(T) + \lambda B_2^{\mathrm{qm},1}(T) + \lambda^2 B_2^{\mathrm{qm},2}(T), \quad (9)$$

where $\lambda = \hbar^2 \beta / 12m$, $\beta = (k_B T)^{-1}$, m is the average isotopic mass of naturally occurring xenon, and $\hbar$ is Planck's constant divided by 2π. The explicit formulae for $B_2^{\mathrm{cl}}(T)$, $B_2^{\mathrm{qm},1}(T)$, and $B_2^{\mathrm{qm},2}(T)$ are summarized, for example, in Ref. 13 and are therefore not repeated here. All integrals needed to compute $B_2(T)$ were solved by means of standard numerical integration methods. The contribution of the second-order quantum correction $\lambda^2 B_2^{\mathrm{qm},2}$ is extremely small. Even at the lowest temperature considered here, $T = 100$ K, it amounts to only –0.011 cm^3 mol^{-1} or about 0.001%. Calculated values of B_2 at temperatures up to 5000 K are listed in the supplementary material along with their estimated uncertainties, which were obtained utilizing the perturbed potentials (see Sec. IV).

In Fig. 1, the values calculated using the present potential are compared with selected experimental data,[60–65] with the correlation of Dymond *et al.*,[66] and with values calculated using the potentials of Aziz and Slaman,[24] of Dham *et al.*,[25] of Slavíček *et al.*,[19] and of Hanni *et al.*[20] The figure shows that the agreement between the values for the present potential and those for the two empirical ones[24,25] is excellent. Only at the very lowest temperatures, the larger well depths of the latter result in slightly more negative values for the second virial coefficient. In contrast, the potential of Slavíček *et al.* yields

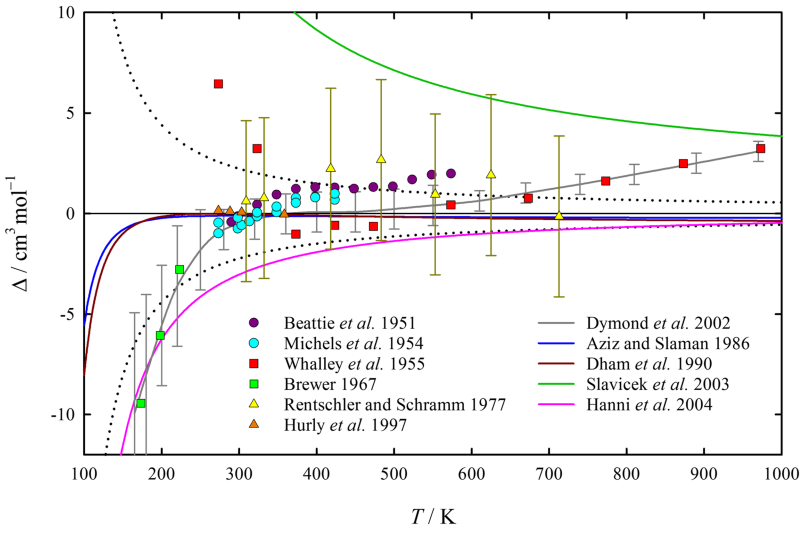

FIG. 1. Deviations, $\Delta = B_2 - B_{2,\mathrm{calc}}$, of selected experimental data,[60–65] of the correlation of Dymond *et al.*,[66] and of values obtained using pair potentials from the literature[19,20,24,25] for the second virial coefficient of xenon from values calculated using the present potential energy curve as a function of temperature. The dotted lines indicate the uncertainty interval of the present values.

values that are clearly too positive due to its underestimated well depth, whereas the values obtained using the potential of Hanni *et al.* are somewhat too negative. It can also be seen that the scatter of the experimental data is much larger than the deviations between the present results and those for the two empirical potentials. We believe that the most accurate data set is that of Hurly *et al.*[65] for temperatures from 273 K to 358 K, which was obtained from both $p\rho T$ measurements with a Burnett apparatus and speed-of-sound measurements and is also the most recent one. Their data deviate from our values by at most 0.15 $\mathrm{cm^3\ mol^{-1}}$, which is more than an order of magnitude smaller than the uncertainty estimates of our values in this temperature range obtained from the perturbed potentials. The figure also shows that Dymond *et al.*[66] based their correlation solely on the available experimental data and not on values obtained from the empirical potentials. The uncertainty estimates given by Dymond *et al.*, which correspond to expanded uncertainties with $k = 2$, are far too optimistic at the highest temperatures.

B. Transport properties

The shear viscosity η, the thermal conductivity λ, and the product of molar density and self-diffusion coefficient, $\rho_{\mathrm{m}} D_{\mathrm{self}}$, of naturally occurring xenon (approximated as a pure gas) in the low-density limit were calculated using the kinetic theory of monatomic gases.[67] All three properties were computed in the fifth-order approximation using formulations in terms of generalized cross sections $\mathfrak{S}\binom{ps}{ps'}$,[4,12,68] which can be related to the more traditional collision integrals $\Omega^{(l,m)}$,[67] see Ref. 12 and references therein for details. We calculated the collision integrals classically using a modified version of the program code developed by O'Hara and Smith.[69,70] All computed transport property values are converged to within 0.001% with respect to the order of the kinetic theory approximation. Calculated values with estimated uncertainties (again obtained from the perturbed potentials) at temperatures from 100 K to 5000 K are provided in the supplementary material.

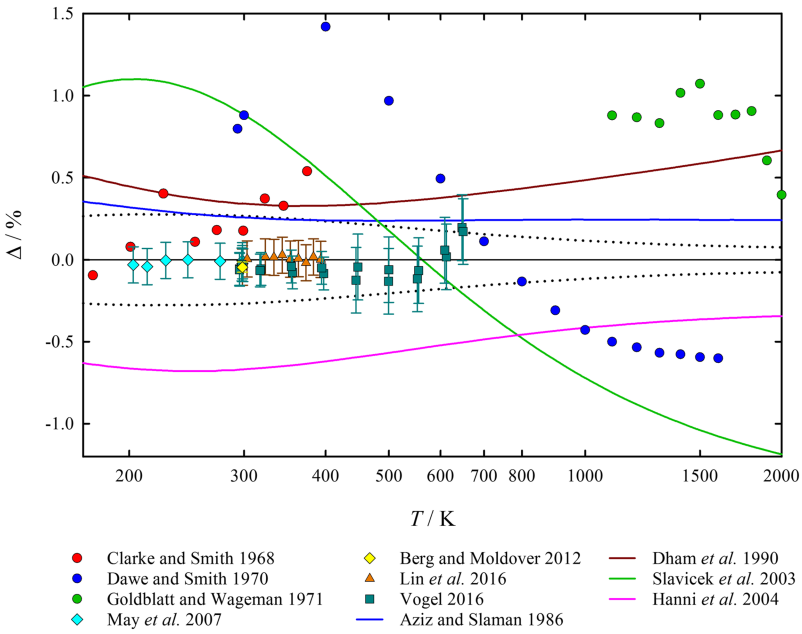

FIG. 2. Relative deviations, $\Delta = (\eta - \eta_{\mathrm{calc}})/\eta_{\mathrm{calc}}$, of selected experimental data,[71–76] of a recommended value at 298.15 K by Berg and Moldover,[5] and of values obtained using pair potentials from the literature[19,20,24,25] for the shear viscosity of dilute xenon from values calculated using the present potential energy curve as a function of temperature. The dotted lines indicate the uncertainty interval of the present values.

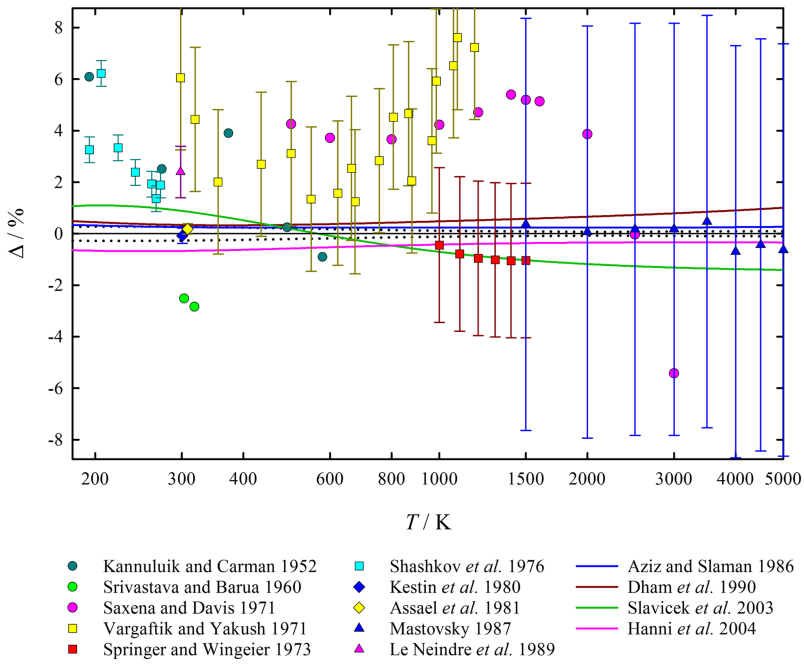

FIG. 3. Relative deviations, $\Delta = (\lambda - \lambda_{calc})/\lambda_{calc}$, of selected experimental data[79–88] and of values obtained using pair potentials from the literature[19,20,24,25] for the thermal conductivity of dilute xenon from values calculated using the present potential energy curve as a function of temperature. The dotted lines indicate the uncertainty interval of the present values.

In Fig. 2, the viscosity values obtained using the present potential energy curve are compared with selected experimental data,[71–76] with a recommended value at 298.15 K by Berg and Moldover,[5] and with values determined using the potentials of Aziz and Slaman,[24] of Dham *et al.*,[25] of Slavíček *et al.*,[19] and of Hanni *et al.*[20] The most accurate data sets are those of May *et al.*,[74] of Lin *et al.*,[75] and of Vogel.[76] Only the viscosity values obtained using the present potential are fully consistent with these three data sets within the experimental uncertainty; the agreement with the data of May *et al.* and of Lin *et al.* is essentially perfect. The data of Vogel, which were obtained by a reanalysis of measurements published in 1984,[77] have a noticeably different temperature dependence at the two highest temperatures. This is due to problems with the thermostat[78] and also affected the measurements at the two highest temperatures for argon and krypton from the same paper[77] (as can be seen in Fig. 4 of Ref. 14 and in Fig. 3 of Ref. 12, respectively). All later measurements with the same instrument were performed using an improved thermostat and are therefore not affected by this problem.[78]

Berg and Moldover[5] critically reviewed reliable viscosity data from the literature for dilute xenon near 298.15 K and corrected them to zero density. They used viscosity ratios related to different gases and anchored them to the *ab initio* viscosity value for helium.[3] Their recommended value has a standard uncertainty of only 0.031% and differs from our value by −0.045%. In contrast, the values for the potentials of Aziz and Slaman,[24] of Dham *et al.*,[25] of Slavíček *et al.*,[19] and of Hanni *et al.*[20] differ from our value by +0.26%, +0.34%, +0.89%, and −0.67%, respectively.

In Figs. 3 and 4, selected experimental data for the thermal conductivity[79–88] and the few available experimental data for the product of molar density and self-diffusion coefficient,[89–91] respectively, are compared with the corresponding values obtained using the present potential and the four potentials from the literature.[19,20,24,25] The relative differences between the thermal conductivity results for the different potentials are almost identical to those obtained for the shear viscosity since both properties are directly linked in the first-order kinetic theory approximation for monatomic gases.[67] Such a link does not exist between the self-diffusion coefficient and the other two properties, but the relative differences are still similar. It is clear from the two figures that an assessment of the quality of the potential energy curves based on a comparison with experimental data is almost impossible due to the much lower accuracy of the available data compared with those for viscosity. The only exceptions are the two thermal conductivity data points close to room temperature of Kestin *et al.*[85] and of Assael *et al.*,[86] which were obtained by means of the transient

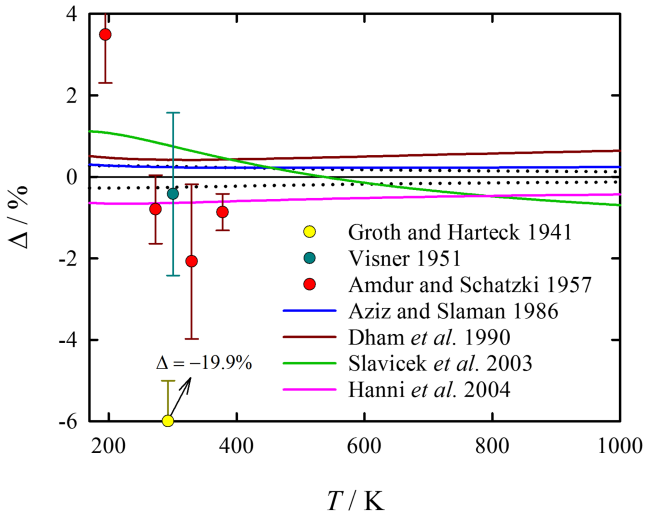

FIG. 4. Relative deviations, $\Delta = (\rho_m D_{self} - \rho_m D_{self,calc})/\rho_m D_{self,calc}$, of the available experimental data[89–91] and of values obtained using pair potentials from the literature[19,20,24,25] for the product of molar density and self-diffusion coefficient of dilute xenon from values calculated using the present potential energy curve as a function of temperature. The dotted lines indicate the uncertainty interval of the present values.

hot-wire technique with claimed uncertainties of 0.3% and 0.2%, respectively. Only the present potential energy curve yields values that agree with both data points within these uncertainties.

VI. SUMMARY AND CONCLUSIONS

A new *ab initio* potential energy curve for the xenon atom pair in the electronic ground state has been developed. It is based on supermolecular CCSD(T) calculations for 39 interatomic separations using newly developed basis sets up to sextuple-zeta quality. Corrections for scalar, spin-(own)-orbit, and spin-other-orbit relativistic effects were determined by a combination of DPT2 and four-component Dirac–Coulomb and Dirac–Coulomb–Gaunt calculations at the CCSD(T) level. Furthermore, corrections for higher coupled-cluster levels up to CCSDTQ were computed nonrelativistically. The two previous *ab initio* potential energy curves for this system,[19,20] which were published more than a decade ago, are based on supermolecular CCSD(T) calculations using only basis sets up to quadruple-zeta quality and employing the less accurate PP approach to account for relativistic effects.

A modified Tang–Toennies function[54] was fitted to the calculated interaction energies. It is characterized by a well depth of $D_e = (279.98 \pm 2.52)$ K and an equilibrium bond length of $R_e = (4.3780 \pm 0.0036)$ Å. The new potential function as well as the two previous *ab initio* potential functions[19,20] and the two most popular empirical ones[24,25] were used to compute the vibrational spectrum of the xenon dimer, the second virial coefficient, and the dilute gas transport properties. From the comparison with the best available experimental data for these properties and for the equilibrium bond length, we conclude that the new potential function is by far the most accurate representation of the Xe–Xe interaction potential to date. In fact, it appears to be of similar quality as our *ab initio* potential functions for the less challenging systems Ne–Ne,[8,13] Ar–Ar,[9,14] and Kr–Kr.[12]

SUPPLEMENTARY MATERIAL

See supplementary material for the exponents and contraction coefficients of the basis sets employed in this work, for detailed results of the quantum-chemical *ab initio* calculations at all 39 investigated interatomic separations, for the parameters of the perturbed potentials, and for calculated values of $\Delta G_{v+1/2}$ for all isotopic combinations and of the second virial coefficient and the dilute gas transport properties of naturally occurring xenon at temperatures from 100 K to 5000 K.

ACKNOWLEDGMENTS

We thank Professor Eckhard Vogel (Universität Rostock) and Dr. Paul Jerabek (Massey University) for helpful discussions.

[1] R. Hellmann, E. Bich, and E. Vogel, Mol. Phys. **105**, 3013 (2007).
[2] E. Bich, R. Hellmann, and E. Vogel, Mol. Phys. **105**, 3035 (2007).
[3] W. Cencek, M. Przybytek, J. Komasa, J. B. Mehl, B. Jeziorski, and K. Szalewicz, J. Chem. Phys. **136**, 224303 (2012).
[4] E. Bich, J. B. Mehl, and R. Hellmann, in *Experimental Thermodynamics Volume IX: Advances in Transport Properties of Fluids*, edited by M. J. Assael, A. R. H. Goodwin, V. Vesovic, and W. A. Wakeham (The Royal Society of Chemistry, Cambridge, 2014), Chap. 7.1, pp. 226–233.
[5] R. F. Berg and M. R. Moldover, J. Phys. Chem. Ref. Data **41**, 043104 (2012).
[6] R. F. Berg and W. C. Burton, Mol. Phys. **111**, 195 (2013).
[7] A. A. H. Pádua, D. Tomida, C. Yokoyama, E. H. Abramson, R. F. Berg, E. F. May, M. R. Moldover, and A. Laesecke, in *Experimental Thermodynamics Volume IX: Advances in Transport Properties of Fluids*, edited by M. J. Assael, A. R. H. Goodwin, V. Vesovic, and W. A. Wakeham (The Royal Society of Chemistry, Cambridge, 2014), Chap. 4, pp. 96–131.
[8] R. Hellmann, E. Bich, and E. Vogel, Mol. Phys. **106**, 133 (2008).
[9] B. Jäger, R. Hellmann, E. Bich, and E. Vogel, Mol. Phys. **107**, 2181 (2009); Corrigendum, **108**, 105 (2010).
[10] K. Patkowski and K. Szalewicz, J. Chem. Phys. **133**, 094304 (2010).
[11] J. M. Waldrop, B. Song, K. Patkowski, and X. Wang, J. Chem. Phys. **142**, 204307 (2015).
[12] B. Jäger, R. Hellmann, E. Bich, and E. Vogel, J. Chem. Phys. **144**, 114304 (2016).
[13] E. Bich, R. Hellmann, and E. Vogel, Mol. Phys. **106**, 1107 (2008).
[14] E. Vogel, B. Jäger, R. Hellmann, and E. Bich, Mol. Phys. **108**, 3335 (2010).
[15] B. Song, X. Wang, and Z. Liu, Mol. Simul. **42**, 9 (2016).
[16] C. Hättig and B. A. Hess, J. Phys. Chem. **100**, 6243 (1996).
[17] N. Runeberg and P. Pyykkö, Int. J. Quantum Chem. **66**, 131 (1998).
[18] S. Faas, J. H. van Lenthe, and J. G. Snijders, Mol. Phys. **98**, 1467 (2000).
[19] P. Slavíček, R. Kalus, P. Paška, I. Odvárková, P. Hobza, and A. Malijevský, J. Chem. Phys. **119**, 2102 (2003).
[20] M. Hanni, P. Lantto, N. Runeberg, J. Jokisaari, and J. Vaara, J. Chem. Phys. **121**, 5908 (2004).
[21] A. Shee, S. Knecht, and T. Saue, Phys. Chem. Chem. Phys. **17**, 10978 (2015).
[22] S. F. Boys and F. Bernardi, Mol. Phys. **19**, 553 (1970).
[23] K. Raghavachari, G. W. Trucks, J. A. Pople, and M. Head-Gordon, Chem. Phys. Lett. **157**, 479 (1989).
[24] R. A. Aziz and M. J. Slaman, Mol. Phys. **57**, 825 (1986).
[25] A. K. Dham, W. J. Meath, A. R. Allnatt, R. A. Aziz, and M. J. Slaman, Chem. Phys. **142**, 173 (1990).
[26] S. A. Kucharski and R. J. Bartlett, Theor. Chim. Acta **80**, 387 (1991).
[27] N. Oliphant and L. Adamowicz, J. Chem. Phys. **95**, 6645 (1991).
[28] T. H. Dunning, Jr., J. Chem. Phys. **90**, 1007 (1989).
[29] R. A. Kendall, T. H. Dunning, Jr., and R. J. Harrison, J. Chem. Phys. **96**, 6796 (1992).
[30] D. E. Woon and T. H. Dunning, Jr., J. Chem. Phys. **99**, 1914 (1993).
[31] A. K. Wilson, T. van Mourik, and T. H. Dunning, Jr., J. Mol. Struct.: THEOCHEM **388**, 339 (1996).
[32] T. van Mourik, A. K. Wilson, and T. H. Dunning, Jr., Mol. Phys. **96**, 529 (1999).
[33] A. K. Wilson, D. E. Woon, K. A. Peterson, and T. H. Dunning, Jr., J. Chem. Phys. **110**, 7667 (1999).
[34] T. Van Mourik and T. H. Dunning, Jr., Int. J. Quantum Chem. **76**, 205 (2000).
[35] T. H. Dunning, Jr., K. A. Peterson, and A. K. Wilson, J. Chem. Phys. **114**, 9244 (2001).
[36] K. A. Peterson and T. H. Dunning, Jr., J. Chem. Phys. **117**, 10548 (2002).
[37] N. J. DeYonker, K. A. Peterson, and A. K. Wilson, J. Phys. Chem. A **111**, 11383 (2007).
[38] K. A. Peterson, D. Figgen, E. Goll, H. Stoll, and M. Dolg, J. Chem. Phys. **119**, 11113 (2003).
[39] D. H. Bross and K. A. Peterson, Theor. Chem. Acc. **133**, 1434 (2014).
[40] A. Mahler and A. K. Wilson, J. Chem. Phys. **142**, 084102 (2015).
[41] E. J. Bylaska, W. A. de Jong, N. Govind, K. Kowalski, T. P. Straatsma, M. Valiev, D. Wang, E. Apra, T. L. Windus, J. Hammond, P. Nichols, S. Hirata, M. T. Hackler, Y. Zhao, P.-D. Fan, R. J. Harrison, M. Dupuis, D. M. A. Smith, J. Nieplocha, V. Tipparaju, M. Krishnan, Q. Wu, T. Van Voorhis, A. A. Auer, M. Nooijen, E. Brown, G. Cisneros, G. I. Fann, H. Fruchtl, J. Garza, K. Hirao, R. Kendall, J. A. Nichols, K. Tsemekhman, K. Wolinski, J. Anchell, D. Bernholdt, P. Borowski, T. Clark, D. Clerc, H. Dachsel, M. Deegan, K. Dyall, D. Elwood, E. Glendening, M. Gutowski, A. Hess, J. Jaffe, B. Johnson, J. Ju, R. Kobayashi, R. Kutteh, Z. Lin, R. Littlefield, X. Long, B. Meng, T. Nakajima, S. Niu, L. Pollack, M. Rosing, G. Sandrone, M. Stave, H. Taylor, G. Thomas, J. van Lenthe, A. Wong, and Z. Zhang, NWChem, a computational chemistry package for parallel computers, version 5.1, Pacific Northwest National Laboratory, Richland, WA, 2007.
[42] T. D. Crawford, C. D. Sherrill, E. F. Valeev, J. T. Fermann, R. A. King, M. L. Leininger, S. T. Brown, C. L. Janssen, E. T. Seidl, J. P. Kenny, and W. D. Allen, J. Comput. Chem. **28**, 1610 (2007).

[43]A. Halkier, T. Helgaker, P. Jørgensen, W. Klopper, H. Koch, J. Olsen, and A. K. Wilson, Chem. Phys. Lett. **286**, 243 (1998).
[44]CFOUR, Coupled-Cluster techniques for Computational Chemistry, a quantum-chemical program package by J. F. Stanton, J. Gauss, M. E. Harding, and P. G. Szalay with contributions from A. A. Auer, R. J. Bartlett, U. Benedikt, C. Berger, D. E. Bernholdt, Y. J. Bomble, L. Cheng, O. Christiansen, M. Heckert, O. Heun, C. Huber, T.-C. Jagau, D. Jonsson, J. Jusélius, K. Klein, W. J. Lauderdale, D. A. Matthews, T. Metzroth, L. A. Mück, D. P. O'Neill, D. R. Price, E. Prochnow, C. Puzzarini, K. Ruud, F. Schiffmann, W. Schwalbach, S. Stopkowicz, A. Tajti, J. Vázquez, F. Wang, and J. D. Watts, and the integral packages MOLECULE (J. Almlöf and P. R. Taylor), PROPS (P. R. Taylor), ABACUS (T. Helgaker, H. J. Aa. Jensen, P. Jørgensen, and J. Olsen), and ECP routines by A. V. Mitin and C. van Wüllen. For the current version, see http://www.cfour.de.
[45]W. Kutzelnigg, E. Ottschofski, and R. Franke, J. Chem. Phys. **102**, 1740 (1995).
[46]W. Klopper, J. Comput. Chem. **18**, 20 (1997).
[47]J. Sikkema, L. Visscher, T. Saue, and M. Iliaš, J. Chem. Phys. **131**, 124116 (2009).
[48]DIRAC, a relativistic *ab initio* electronic structure program, Release DIRAC14, 2014, written by T. Saue, L. Visscher, H. J. Aa. Jensen, and R. Bast, with contributions from V. Bakken, K. G. Dyall, S. Dubillard, U. Ekström, E. Eliav, T. Enevoldsen, E. Faßhauer, T. Fleig, O. Fossgaard, A. S. P. Gomes, T. Helgaker, J. K. Lærdahl, Y. S. Lee, J. Henriksson, M. Iliaš, Ch. R. Jacob, S. Knecht, S. Komorovský, O. Kullie, C. V. Larsen, H. S. Nataraj, P. Norman, G. Olejniczak, J. Olsen, Y. C. Park, J. K. Pedersen, M. Pernpointner, R. di Remigio, K. Ruud, P. Sałek, B. Schimmelpfennig, J. Sikkema, A. J. Thorvaldsen, J. Thyssen, J. van Stralen, S. Villaume, O. Visser, T. Winther, and S. Yamamoto (see http://www.diracprogram.org).
[49]J. Noga and R. J. Bartlett, J. Chem. Phys. **86**, 7041 (1987); Erratum, **89**, 3401 (1988).
[50]Y. J. Bomble, J. F. Stanton, M. Kállay, and J. Gauss, J. Chem. Phys. **123**, 054101 (2005).
[51]M. Kállay and J. Gauss, J. Chem. Phys. **123**, 214105 (2005).
[52]D. A. Matthews and J. F. Stanton, J. Chem. Phys. **142**, 064108 (2015).
[53]MRCC, a string-based general coupled cluster program suite written by M. Kállay. See also M. Kállay and P. R. Surján, J. Chem. Phys. **115**, 2945 (2001), as well as: http://www.mrcc.hu.
[54]K. T. Tang and J. P. Toennies, J. Chem. Phys. **80**, 3726 (1984).
[55]A. Kumar and A. J. Thakkar, J. Chem. Phys. **132**, 074301 (2010).
[56]A. Wüest, U. Hollenstein, K. G. de Bruin, and F. Merkt, Can. J. Chem. **82**, 750 (2004).
[57]R. J. Le Roy, "LEVEL 7.7: A computer program for solving the radial Schrödinger equation for bound and quasibound levels," University of Waterloo Chemical Physics Research Report No. CP-661, University of Waterloo, Waterloo, Ontario, Canada, 2005.
[58]D. E. Freeman, K. Yoshino, and Y. Tanaka, J. Chem. Phys. **61**, 4880 (1974).
[59]S. Valkiers, Y. Aregbe, P. D. P. Taylor, and P. De Bièvre, Int. J. Mass Spectrom. Ion Processes **173**, 55 (1998).
[60]J. A. Beattie, R. J. Barriault, and J. S. Brierley, J. Chem. Phys. **19**, 1222 (1951).
[61]A. Michels, T. Wassenaar, and P. Louwerse, Physica **20**, 99 (1954).
[62]E. Whalley, Y. Lupien, and W. G. Schneider, Can. J. Chem. **33**, 633 (1955).
[63]J. Brewer, Technical Report No. 67–2795, AFOSR, 1967.
[64]H.-P. Rentschler and B. Schramm, Ber. Bunsenges. Phys. Chem. **81**, 319 (1977).
[65]J. J. Hurly, J. W. Schmidt, S. J. Boyes, and M. R. Moldover, Int. J. Thermophys. **18**, 579 (1997).
[66]J. H. Dymond, K. N. Marsh, R. C. Wilhoit, and K. C. Wong, in *Landolt-Börnstein: Numerical Data and Functional Relationships in Science and Technology: New Series*, Group IV: Physical Chemistry, Vol. 21A, edited by M. Frenkel and K. N. Marsh (Springer, Berlin, Heidelberg, New York, 2002), Chap. 2, p. 79.
[67]S. Chapman and T. G. Cowling, *The Mathematical Theory of Non-Uniform Gases*, 3rd ed. (Cambridge University Press, Cambridge, 1970).
[68]F. R. W. McCourt, J. J. M. Beenakker, W. E. Köhler, and I. Kuščer, *Nonequilibrium Phenomena in Polyatomic Gases, Vol. I: Dilute Gases* (Clarendon Press, Oxford, 1990).
[69]H. O'Hara and F. J. Smith, J. Comput. Phys. **5**, 328 (1970).
[70]H. O'Hara and F. J. Smith, Comput. Phys. Commun. **2**, 47 (1971).
[71]A. G. Clarke and E. B. Smith, J. Chem. Phys. **48**, 3988 (1968).
[72]R. A. Dawe and E. B. Smith, J. Chem. Phys. **52**, 693 (1970).
[73]M. Goldblatt and W. E. Wageman, Phys. Fluids **14**, 1024 (1971).
[74]E. F. May, R. F. Berg, and M. R. Moldover, Int. J. Thermophys. **28**, 1085 (2007).
[75]H. Lin, J. Che, J. T. Zhang, and X. J. Feng, Fluid Phase Equilib. **418**, 198 (2016).
[76]E. Vogel, Int. J. Thermophys. **37**, 63 (2016).
[77]E. Vogel, Ber. Bunsenges. Phys. Chem. **88**, 997 (1984).
[78]E. Vogel, private communication (2017).
[79]W. G. Kannuluik and E. H. Carman, Proc. Phys. Soc., London, Sect. B **65**, 701 (1952).
[80]B. N. Srivastava and A. K. Barua, J. Chem. Phys. **32**, 427 (1960).
[81]S. C. Saxena and F. E. Davis, J. Phys. E **4**, 681 (1971).
[82]N. B. Vargaftik and L. V. Yakush, J. Eng. Phys. **21**, 1156 (1971).
[83]G. S. Springer and E. W. Wingeier, J. Chem. Phys. **59**, 2747 (1973).
[84]A. G. Shashkov, N. A. Nesterov, V. M. Sudnik, and V. I. Aleinikova, J. Eng. Phys. **30**, 439 (1976).
[85]J. Kestin, R. Paul, A. A. Clifford, and W. A. Wakeham, Physica A **100**, 349 (1980).
[86]M. J. Assael, M. Dix, A. Lucas, and W. A. Wakeham, J. Chem. Soc., Faraday Trans. 1 **77**, 439 (1981).
[87]J. Maštovský, Technical Report No. Z–1026/87, ČSAV, Ústav Termomechaniky, Prague, 1987.
[88]B. Le Neindre, Y. Garrabos, and R. Tufeu, Physica A **156**, 512 (1989).
[89]W. Groth and P. Harteck, Z. Elektrochem. Angew. Physik. Chem. **47**, 167 (1941).
[90]S. Visner, in "Proceedings of the American Physical Society," Phys. Rev. **82**, 291 (1951).
[91]I. Amdur and T. F. Schatzki, J. Chem. Phys. **27**, 1049 (1957).